



HAL
open science

Numerical investigation of the maximum thermoelectric efficiency

Patrice Limelette

► **To cite this version:**

Patrice Limelette. Numerical investigation of the maximum thermoelectric efficiency. AIP Advances, 2021, 11, 10.1063/5.0041224 . hal-03192476

HAL Id: hal-03192476

<https://univ-tours.hal.science/hal-03192476>

Submitted on 8 Apr 2021

HAL is a multi-disciplinary open access archive for the deposit and dissemination of scientific research documents, whether they are published or not. The documents may come from teaching and research institutions in France or abroad, or from public or private research centers.

L'archive ouverte pluridisciplinaire **HAL**, est destinée au dépôt et à la diffusion de documents scientifiques de niveau recherche, publiés ou non, émanant des établissements d'enseignement et de recherche français ou étrangers, des laboratoires publics ou privés.

Numerical investigation of the maximum thermoelectric efficiency

Cite as: AIP Advances 11, 035135 (2021); <https://doi.org/10.1063/5.0041224>

Submitted: 01 March 2021 . Accepted: 05 March 2021 . Published Online: 19 March 2021

 Patrice Limelette



[View Online](#)



[Export Citation](#)



[CrossMark](#)

AIP Advances **Photonics and Optics Collection**

[READ NOW!](#)

Numerical investigation of the maximum thermoelectric efficiency

Cite as: AIP Advances 11, 035135 (2021); doi: 10.1063/5.0041224

Submitted: 1 March 2021 • Accepted: 5 March 2021 •

Published Online: 19 March 2021



View Online



Export Citation



CrossMark

Patrice Limelette^{a)}

AFFILIATIONS

GREMAN, UMR 7347 CNRS-INSA-Université de Tours, Parc de Grandmont, 37200 Tours, France

^{a)} Author to whom correspondence should be addressed: patrice.limelette@univ-tours.fr

ABSTRACT

The maximum thermoelectric efficiency that is given by the so-called dimensionless figure of merit ZT is investigated here numerically for various energy dependence. By involving the electrical conductivity σ , the thermopower α , and the thermal conductivity κ such that $ZT = \alpha^2 \times \sigma \times T / \kappa$, the figure of merit is computed in the frame of a semiclassical approach that implies Fermi integrals. This formalism allows us to take into account the full energy dependence in the transport integrals through a previously introduced exponent s that combines the energy dependence of the quasiparticles' velocity, the density of states, and the relaxation time. While it has been shown that an unconventional exponent $s = 4$ was relevant in the context of the conducting polymers, the question of the maximum of ZT is addressed by varying s from 1 up to 4 through a materials quality factor analysis. In particular, it is found that the exponent $s = 4$ allows for an extended range of high figure of merit toward the slightly degenerate regime. Useful analytical asymptotic relations are given, and a generalization of the Chasmar and Stratton formula of ZT is also provided.

© 2021 Author(s). All article content, except where otherwise noted, is licensed under a Creative Commons Attribution (CC BY) license (<http://creativecommons.org/licenses/by/4.0/>). <https://doi.org/10.1063/5.0041224>

Discovered nearly two centuries ago, the thermoelectric effects that allow for the conversion of heat waste into electricity¹ are nowadays a potential part of the strategy to meet sustainable development.^{2,3} They have been widely investigated during the 1960s,^{4–7} and a renewed interest appeared in the last decades likely due to the environmental concern and the growing number of new complex materials.^{1,8–10} In this context, organic materials such as conducting polymers¹¹ have been identified^{12,13} as potential promising candidates to compete with conventional inorganic thermoelectric materials.¹⁴ With their low cost, abundant elements, large processability, and flexibility, they could bring new opportunities to develop unexpected applications such as thermoelectric textiles, for instance.¹⁵ Furthermore, the spectacular results reported in some conducting polymers^{14,16} with high thermoelectric efficiency have stimulated more systematically both electrical conductivity and thermopower measurements.^{17–19} In particular, an unconventional scaling relation between the thermopower and the electrical conductivity such that $\alpha \propto \sigma^{-1/s}$ with $s = 4$ has been pointed out by several groups in a wide variety of conducting polymers as a function of doping.^{20–23} While some models have accounted for this quasi-universal law over a restricted range of parameters,²⁴ a successful demonstration of the latter power law has been given in the frame of a charge transport

model with $s = 3$.²⁵ More recently, this approach has been extended in order to explain the exponent $s = 4$ by considering that charge carriers could behave as Dirac quasiparticles, namely, massless pseudo-relativistic particles.²⁶ This has required us to take into account all the energy dependence in the transport integrals by showing that s is, in fact, the sum of the exponents of the power law energy dependence of the relaxation time τ_E , the quasiparticles' velocity $v_{x,E}$, and the density of states g_E as defined in the following:

$$\tau_E = \tau_0 \times (E/E_\tau)^\theta, \quad v_{x,E}^2 = v_0^2 \times (E/E_v)^\nu, \\ g_E = g_0 \times (E/E_g)^\gamma.$$

Then, it has been demonstrated that $s = (\theta + \nu + \gamma)$. The characteristic energies E_τ , E_v , and E_g and the constants τ_0 , v_0 , and g_0 have been introduced in order to focus on energy dependence.²⁶ In the frame of this formalism, the semi-classical treatment of the Boltzmann equation^{25,26} allows us to formulate the transport coefficients in terms of Fermi integrals $F_s(\tilde{\mu})$, which include both non-degenerate (insulating) and degenerate (metallic) regimes. In particular, the electrical conductivity σ and the thermopower α can be written as a function of $F_s(\tilde{\mu})$ according to Eq. (1), with the reduced chemical potential $\tilde{\mu} = \mu/k_B T$,

$$\sigma = \sigma_{E_0} \times s \times F_{s-1}(\tilde{\mu}), \quad \alpha = \frac{k_B}{q} \left(\frac{(s+1) \times F_s(\tilde{\mu})}{s \times F_{s-1}(\tilde{\mu})} - \tilde{\mu} \right),$$

with

$$F_s(\tilde{\mu}) = \int_0^\infty \frac{x^s}{e^{x-\tilde{\mu}} + 1} dx, \quad (1)$$

whereas some approximations of Fermi integrals $F_s(\tilde{\mu})$ provide analytical relations if $|\tilde{\mu}| \gg 1$; these general formulations are especially useful in order to investigate numerically the transport coefficients in the intermediate regime.

For non-relativistic free electrons ($\nu = 1$) in three dimensions ($\gamma = 1/2$), it follows that $s = 3/2 + \theta$. If they are scattered by acoustic phonons above the Debye temperature or by screened ionized impurities, then $\theta = -1/2$ and $s = 1$.⁶ If they undergo polar scattering from optical phonons, then $\theta = 1/2$ and $s = 2$,²⁷ and if they are scattered by unscreened ionized impurities, then $\theta = 3/2$ and $s = 3$.^{25,26} In addition, it has been shown that, for Dirac quasiparticles ($\nu = 0$) in three dimensions ($\gamma = 2$), the relaxation time due to scattering by unscreened ionized impurities varies quadratically as a function of energy, namely, $\theta = 2$ and then $s = 4$.²⁶ Therefore, the general formulations of the transport coefficients according to Eq. (1) allow us to investigate numerically, for different charge carriers, densities of states, and scattering mechanisms, the maximum thermoelectric efficiency as a function of s varying from 1 up to 4 as reported thereafter.

By calculating the Fermi integrals $F_{s-1}(\tilde{\mu})$, the normalized electrical conductivity σ/σ_{E_0} can be computed as a function of the reduced temperature $k_B T/|\mu|$ as displayed in Fig. 1(a) for the various investigated exponents s . Whatever the exponent s is, the insulating behavior is here recovered with the increasing electrical conductivity with temperature ($\mu < 0$) and the metallic one is observed with the decreasing electrical conductivity with temperature ($\mu > 0$). By using the corresponding limits, it can be demonstrated that a standard activated behavior is found for the electrical conductivity in the non-degenerate regime if $\tilde{\mu} \ll -1$, while a power law dependence is expected if $\tilde{\mu} \gg 1$ in the degenerate one,

$$\sigma_{\tilde{\mu} \gg 1} = \sigma_{E_0} \times \tilde{\mu}^s, \quad \sigma_{\tilde{\mu} \ll -1} = \sigma_{E_0} \times \Gamma(s+1) \times e^{\tilde{\mu}}$$

with the well known Γ function. Interestingly, Fig. 1(a) also displays the asymptotic behavior of σ as $\tilde{\mu} \rightarrow 0$ with the convergence of the electrical conductivity from both metallic and insulating sides toward a common value. Thus, the latter indicates the maximum conductivity that can be reached in the insulating state as well as the minimum metallic conductivity.

On the other hand, the use of the corresponding Fermi integrals according to Eq. (1) allows us to plot in Fig. 1(b) the temperature dependence of thermopower, in absolute value, for the various investigated exponents s . Once more, the low temperature behaviors in both regimes are here recovered with the increasing T-linear thermopower in the metallic state if $\tilde{\mu} \gg 1$ and the decreasing thermopower if $\tilde{\mu} \ll -1$ as $1/T$ in the insulating one such that

$$\alpha_{\tilde{\mu} \gg 1} = \frac{\pi^2}{3} \times \frac{k_B}{e} \times \frac{s}{\tilde{\mu}}, \quad \alpha_{\tilde{\mu} \ll -1} = \frac{k_B}{e} \times ((s+1) - \tilde{\mu}).$$

In a close analogy with the electrical conductivity, the thermopower in Fig. 1(b) converges from both metallic and insulating regimes

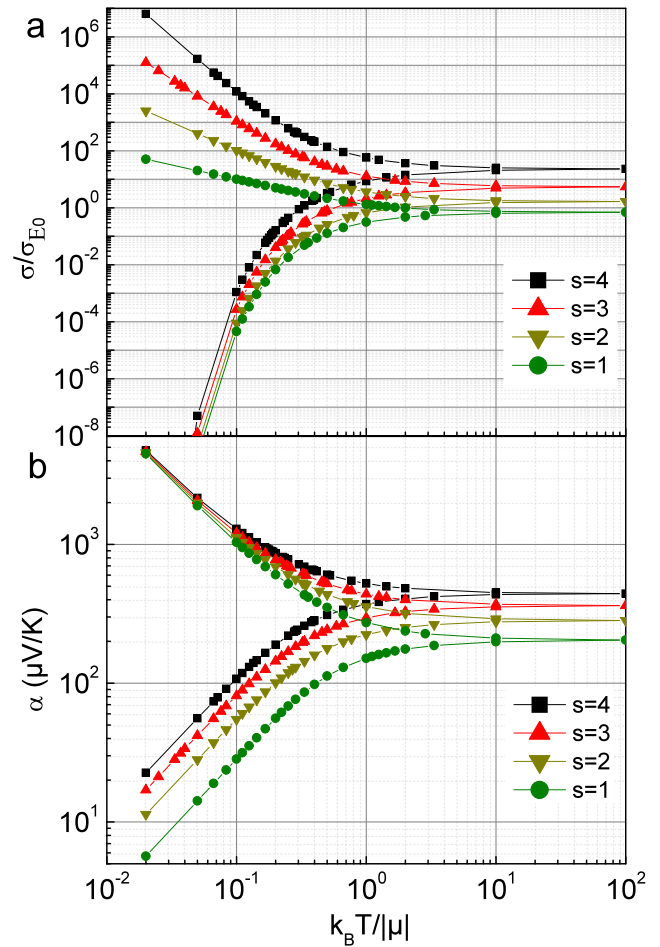


FIG. 1. (a) Normalized electrical conductivity σ/σ_{E_0} and (b) absolute value of the thermopower α as a function of the reduced temperature $k_B T/|\mu|$ for various integer exponents s ranging from 1 up to 4.

toward a common value at high temperatures. The latter asymptotic value is seen to increase with the exponent s from nearly 205 $\mu\text{V}/\text{K}$ for $s = 1$ up to nearly 442 $\mu\text{V}/\text{K}$ for $s = 4$ in the limit $\tilde{\mu} \rightarrow 0$ by illustrating that stronger energy dependence favors higher thermopower. Nevertheless, one must emphasize that a high thermopower is *a priori* not sufficient to reach the best thermoelectric efficiency since the latter involves through the figure of merit ZT two other transport coefficients, namely, both the electrical and thermal conductivities σ and κ .

It is, therefore, of fundamental interest to investigate the Lorentz number that is defined as $L = \kappa_e/(\sigma \times T)$, with the electronic thermal conductivity κ_e , and that can also be related to Fermi integrals in both regimes according to the following equation:²⁵

$$L = \left(\frac{k_B}{e} \right)^2 \times \left[\frac{(s+2) \times F_{s+1}(\tilde{\mu})}{s \times F_{s-1}(\tilde{\mu})} - \frac{(s+1)^2 \times F_s^2(\tilde{\mu})}{s^2 \times F_{s-1}^2(\tilde{\mu})} \right].$$

If $\tilde{\mu} \gg 1$, the Lorentz number recovers, whatever the exponent s is, the well known metallic limit $\pi^2/3 \times (k_B/e)^2$ in agreement with the Wiedemann–Franz law as seen in Fig. 2(a). The power expansion

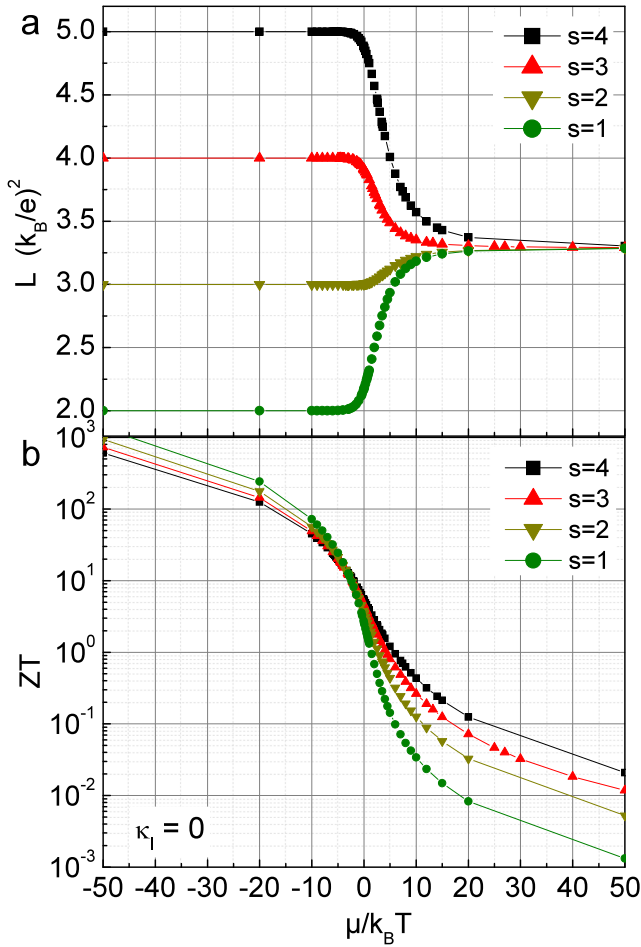


FIG. 2. (a) Dimensionless Lorentz number [in unit of $(k_B/e)^2$] and (b) figure of merit ZT without lattice contribution ($\kappa_l = 0$) as a function of the reduced chemical potential $\tilde{\mu}$ for various integer exponents s ranging from 1 up to 4.

of the Fermi integrals in this strongly degenerate regime allows us to retain the first order correction to the Wiedemann–Franz law as a function of s . This leads to Eq. (2) that accounts for the change in curvature as a function of $\tilde{\mu}$ as displayed in Fig. 2(a) between $s = 1$ or 2 and $s = 3$ or 4. In particular, the lowering of L with decreasing $\tilde{\mu}$ for $s = 1$ is here recovered such that $L_{\tilde{\mu} \gg 1} = \left(\frac{k_B}{e}\right)^2 \times \frac{\pi^2}{3} \times \left(1 - \frac{\pi^2}{3} \times \tilde{\mu}^{-2}\right)$ as emphasized by Fistul.⁶ On the other hand, the equivalent limit in the insulating state is found to be strongly s -dependent. Actually, by considering the approximate form of the Fermi integrals $F_s(\tilde{\mu} \ll -1) \approx \Gamma(s+1) \times e^{\tilde{\mu}}$ combined with the property $\Gamma(s+1) = s \times \Gamma(s)$, one can easily find Eq. (3),

$$L_{\tilde{\mu} \gg 1} = \left(\frac{k_B}{e}\right)^2 \times \frac{\pi^2}{3} \times \left(1 + \frac{\pi^2}{15} \times \frac{s}{\tilde{\mu}^2} \times (3s - 8)\right), \quad (2)$$

$$L_{\tilde{\mu} \ll -1} = (s+1) \times \left(\frac{k_B}{e}\right)^2. \quad (3)$$

The latter equation (3) implies, thus, that the Lorentz number increases with s in the insulating regime as well illustrated in Fig. 2(a) as $(s+1)$. By combining the thermopower displayed in Fig. 1(b) and the Lorentz number in Fig. 2(a), an electronic figure of merit, namely, without lattice thermal conductivity, can be inferred such that $ZT = \alpha^2/L$. It is worth mentioning that, since the Lorentz number does not depend on σ_{E_0} , the latter figure of merit only depends on the reduced chemical potential and the exponent s . The variation of ZT as a function of $\tilde{\mu}$ displayed in Fig. 2(b) represents then a theoretical maximum figure of merit in the frame of the investigated exponents s . It is also interesting to note that, for a given s , the observed behavior is mainly governed by the variation of thermopower with its continuous increase with the decrease in $\tilde{\mu}$ as suggested in Fig. 1(b). The influence of the exponent s is, however, less obvious. Actually, the figure of merit is enhanced for a higher exponent s in the metallic regime due to higher thermopower, but a crossing point appears in the slightly non-degenerate regime from which ZT is higher for lower exponents s . The latter behavior is, in fact, a consequence of the evolution of the Lorentz number in Fig. 2(a) with its noticeable decrease for lower exponents s , while, in the insulating regime, the thermopower tends to be more and more s -independent as $\tilde{\mu}$ decreases ($\alpha_{\tilde{\mu} \ll -1} \rightarrow \frac{k_B}{e} \times |\tilde{\mu}|$). Thus, it results that a higher exponent s will favor a higher figure of merit in the metallic regime, whereas a lower exponent s will favor a higher figure of merit in the insulating regime as suggested from the asymptotic expressions of ZT ,

$$ZT_{\tilde{\mu} \gg 1} = \frac{\pi^2}{3} \times \frac{s^2}{\tilde{\mu}^2}, \quad ZT_{\tilde{\mu} \ll -1} = \frac{((s+1) - \tilde{\mu})^2}{s+1} \rightarrow \frac{\tilde{\mu}^2}{s+1}.$$

Of course, the thermal conductivity of the lattice κ_l needs to be taken into account in real materials and the definition of the figure of merit must include it such that $ZT = \alpha^2 \times \sigma \times T / (\kappa_e + \kappa_l)$. As identified by Chasmar and Stratton earlier,⁴ it may be useful to introduce the so-called material quality factor B as defined in the following equation in order to express the figure of merit:^{25,27}

$$ZT = \frac{\alpha^2}{L + \frac{\kappa_l}{\sigma \times T}}, \quad \text{with } B = \left(\frac{k_B}{e}\right)^2 \times \frac{\sigma_{E_0} \times T}{\kappa_l}. \quad (4)$$

According to its definition, B is dimensionless and the figure of merit will be higher if the material quality factor is as large as possible. It means that the figure of merit will tend to the one displayed in Fig. 2(b) if $B \rightarrow \infty$. Furthermore, the asymptotic expressions of ZT including the material quality factor can be given in both regimes as

$$ZT_{\tilde{\mu} \gg 1} = \frac{\frac{\pi^2}{3} \times s^2 \times \tilde{\mu}^{-2}}{1 + \frac{\pi^2}{15} \times \tilde{\mu}^{-2} \times s \times (3s - 8) + \left(\frac{\pi^2}{3} \times B \times \tilde{\mu}^s\right)^{-1}}, \quad (5)$$

$$ZT_{\tilde{\mu} \ll -1} = \frac{((s+1) - \tilde{\mu})^2}{(s+1) + (B \times e^{\tilde{\mu}} \times \Gamma(s+1))^{-1}}. \quad (6)$$

The above equations appear as a generalization to an arbitrary exponent s of the figure of merit provided by Chasmar and Stratton⁴ earlier with $s = \theta + 3/2$ (note that $\theta = v$ in their original paper). In the degenerate regime, Eq. (5) mainly predicts rather low ZT values, and it should be considered a rough approximation for s higher than 2 because it should require rigorously to include higher order

correction terms in both α and L due to the presence of $\tilde{\mu}^{-s}$ in the denominator. In the non-degenerate regime, Eq. (6) appears able to predict higher ZT values if $\tilde{\mu}$ is only moderately negative, while B is high enough in order to prevent the term $B \times e^{\tilde{\mu}}$ from lowering ZT. In such a condition, ZT will get closer to its previously discussed asymptotic expression and could thus reach values higher than 1. Actually, more negative $\tilde{\mu}$ values would require a huge material quality factor that seems unlikely due to the finite lattice thermal conductivity in the real system. This is the reason that explains why high ZT values cannot be reached in strongly non-degenerate materials.

In order to discuss more quantitatively the thermoelectric efficiency, the figure of merit has been computed for various material quality factors ranging from 7.4×10^{-6} up to 12 for each exponents. Figure 3(a) shows the results obtained for $s = 4$ by including the

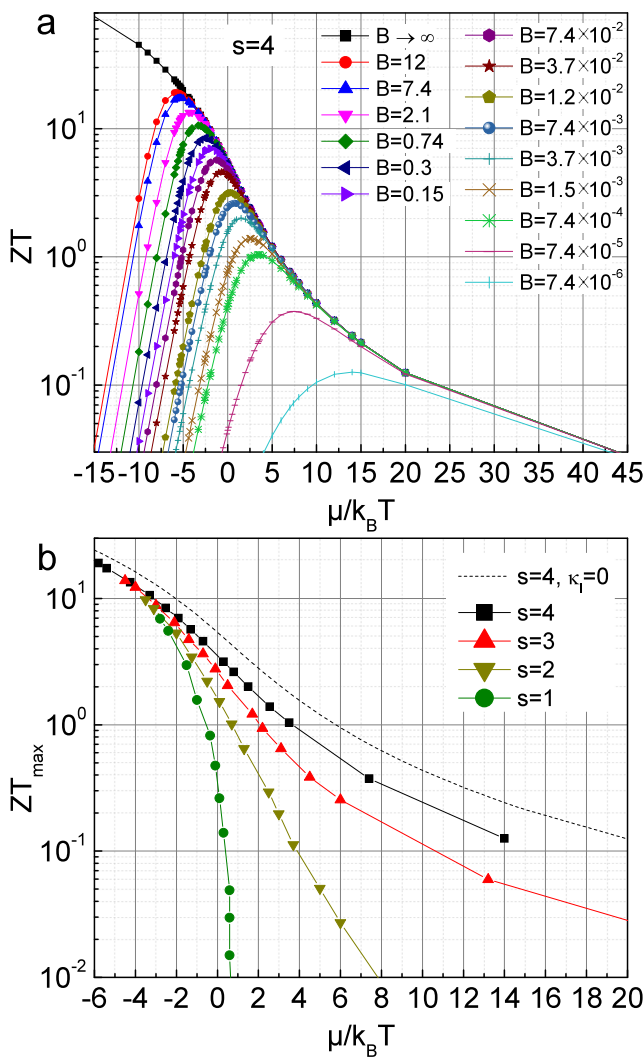


FIG. 3. (a) Figure of merit ZT with $s = 4$ for various material quality factors B and (b) maximum figure of merit ZT_{max} for distinct exponents s as a function of the reduced chemical potential $\tilde{\mu}$. Note that the same material quality factors have been used for the different exponents s .

figure of merit with $B \rightarrow \infty$ as already displayed in Fig. 2(b). These results illustrate the influence of finite material quality factor on ZT, namely, the B -factor basically truncates the increase in the figure of merit with decreasing $\tilde{\mu}$ by inducing a maximum. This effect is even more pronounced if B is low, which leads to lowering the ZT maximum due to a shift toward higher chemical potentials. The overall results are then summarized in Fig. 3(b) by showing the variation of the ZT maximum as a function of $\tilde{\mu}$ for the distinct exponents s investigated. One recovers here the same trend as in Fig. 2(b) with higher ZT maxima in the metallic regime for higher exponents s and a crossing point in the slightly non-degenerate regime around $\tilde{\mu} \approx -4$. It is also demonstrated that the maximum of the figure of merit can only be higher than 1 in an intermediate regime with $|\tilde{\mu}| < 4$, namely, slightly either degenerate or non-degenerate for exponents s up to 4. The restriction to a slightly non-degenerate regime originates from the previously discussed condition concerning $B \times e^{\tilde{\mu}}$, which strongly lowers ZT if $\tilde{\mu}$ is too negative since B cannot be arbitrarily high.

Furthermore, it is also interesting to plot in Fig. 4 the maximum ZT as a function of B in order to compare the values of ZT for a given B as a function of s . This highlights that a larger figure of merit can be reached if s is high for a given B and that a same ZT can be found for higher s with low material quality factor, namely, with higher lattice thermal conductivity, for instance. As displayed in Fig. 4, the highest ZTs are expected for a large material quality factor and values such as $ZT_{max} \approx 20$ could be reached with $B = 12$ for $s = 4$. Since large material quality factors require low κ_l , this raises the question of the lowest accessible lattice thermal conductivity. It is worth mentioning that several successful attempts to calculate the high temperature lattice thermal conductivity have already been made, by including, in particular, the anharmonicity of lattice vibrations.⁵ As a consequence, they involve the Grüneisen parameter²⁸ and the thermal expansion coefficient²⁹ that are not always known, but a simpler approach can be sufficient to discuss the order

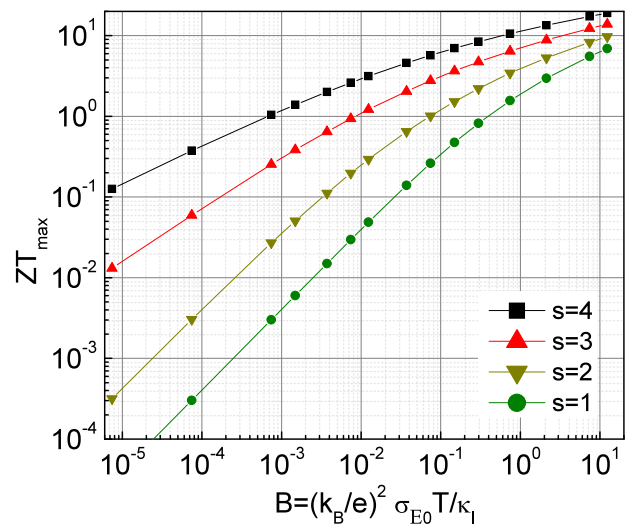


FIG. 4. Maximum figure of merit ZT_{max} as a function of the material quality factor B for various integer exponents s ranging from 1 up to 4.

of magnitude of κ_l . At a classical level, the lattice thermal conductivity is proportional to the specific heat per unit volume C_v , the sound velocity v_s , and the mean free path of phonons l such that $\kappa_l \approx \frac{1}{3} \times C_v \times v_s \times l$. Above the Debye temperature T_D , the specific heat is expected to be constant, and for a mono-atomic cubic unit cell, $C_v = 3 \times k_B/a^3$, with the interatomic spacing a . According to Debye theory, the dispersion relation of acoustic phonons is linear, with v_s as the slope, and then $k_B \times T_D = \hbar \times v_s \times k_D$, with the Debye wave vector $k_D \approx \pi/a$. Note that the latter is actually a bit higher in the Debye model for a cubic lattice, but it is here believed that this approximation is sufficient to discuss the order of magnitude. So, the sound velocity is expected to vary as $v_s \approx 2 \times a \times k_B \times T_D/\hbar$. Since the phonons' mean free path is decreasing with T at high temperature but cannot be lower than the interatomic spacing, one infers that $l \geq a$. By combining these relations, a simple low lattice thermal conductivity limit can be given such that $\kappa_l \geq 2 \times k_B \frac{k_B \times T_D}{\hbar \times a}$. The latter suggests then that low Debye temperature and large interatomic spacing will favor a low lattice thermal conductivity. For instance, if one considers the low value $T_D \approx 50$ K with $a \approx 0.15$ nm, one infers $\kappa_l \geq 0.2$ W m⁻¹ K⁻¹. Despite its simplicity, this result seems to agree quite well with the order of magnitude of the lowest thermal conductivity observed in solids at room temperature³⁰ and also roughly with the measured thermal conductivity in conducting polymers.

By considering now the values of the material quality factor required to reach $ZT_{max} = 10$, namely, from 0.6 for $s = 4$ up to 35 for $s = 1$ (not shown in Fig. 4), one deduces with $\kappa_l \approx 0.2$ W m⁻¹ K⁻¹ the values of the electrical conductivity parameter σ_{E_0} ranging from nearly 5×10^4 S/m for $s = 4$ up to 3×10^6 S/m for $s = 1$. These values allow then to calculate the corresponding electrical conductivity from Fig. 1(a) with the use of the chemical potential associated with ZT_{max} in Fig. 3(b), which lies between -3 and -4 depending on s . Surprisingly, it leads to the nearly common value $\sigma \approx 6 \times 10^4$ S/m ($\rho \approx 1.5$ mΩ cm) at room temperature for whatever s . Even if such a value is rather high for a non-degenerate system, it remains below the Mott minimum metallic conductivity,³¹ and thus, it appears realistic in a slightly non-degenerate material. As a matter of fact, one may emphasize that this is typically the range of the electrical conductivity measured in the conventional thermoelectric materials of the Bi₂Te₃ family. In the case of conducting polymers characterized by the exponent $s = 4$, these results show that the figure of merit will exceed 1 at room temperature if σ_{E_0} is higher than 66 S/m with $\kappa_l \approx 0.2$ W m⁻¹ K⁻¹. In particular, the value $\sigma_{E_0} \approx 0.6$ S/m found in the oriented PBTTT²⁶ is expected to lead to a ZT of the order of 0.1 by optimizing the doping. Even if such a value is still lower than 1, it is very promising and it shows that the electrical conductivity, σ_{E_0} , still needs to be improved in order to reach a higher figure of merit.

Therefore, it seems that values of figure of merit as high as 10 may be reachable experimentally in materials characterized by lattice thermal conductivity of the order of 0.2 W m⁻¹ K⁻¹ by fine-tuning the doping in order to locate the chemical potential between -3 and -4 . This numerical investigation has also demonstrated that higher figures of merit are expected in materials with stronger energy dependence, namely, with a large exponent s , and that their range can extend toward the slightly degenerate regime up to $\tilde{\mu} = 4$ if $s = 4$, for instance. With their low lattice thermal conductivity, large s exponent, and the possibility of fine-tuning the doping, the

conducting polymers appear definitely as very promising thermoelectric materials. The experimental challenge is now to succeed in enhancing even more their electrical conductivity in order to fulfill all the requirements.

The author acknowledges the support from the ANR Anisotherm (Grant No. ANR-17-CE05-0012-04) and from la Région Centre-Val de Loire through the ETHERMO Project (No. 2020-00138653).

DATA AVAILABILITY

The data that support the findings of this study are available from the corresponding author upon reasonable request.

REFERENCES

- G. D. Mahan and J. O. Sofo, *Proc. Natl. Acad. Sci. U. S. A.* **93**, 7436–7439 (1996).
- J. J. Urban, A. K. Menon, Z. Tian, A. Jain, and K. J. Hippalgaonkar, *J. Appl. Phys.* **125**, 180902 (2019).
- A. Zevalkink, D. M. Smiadak, J. L. Blackburn, A. J. Ferguson, M. L. Chabiny, O. Delaire, J. Wang, K. Kovnir, J. Martin, L. T. Schelhas *et al.*, *Appl. Phys. Rev.* **5**, 021303 (2018).
- R. P. Chasmar and R. J. Stratton, *J. Electron. Control* **7**, 52 (1959).
- R. P. Goldsmid, *Thermoelectric Refrigeration* (Plenum Press, 1964).
- V. I. Fistul, *Heavily Doped Semiconductors* (Plenum Press, 1969).
- L. R. Testardi, *J. Appl. Phys.* **32**, 1978 (1961).
- G. D. Mahan, B. Sales, and J. Sharp, *Phys. Today* **50**, 42 (1997).
- G. J. Snyder and E. S. Toberer, *Nat. Mater.* **7**, 106 (2008).
- Y. Yan, Y. R. Jin, G. Zhang, J. Yang, Y. Wang, and W. Ren, *Sci. Rep.* **7**, 10104 (2017).
- A. Heeger, *Rev. Mod. Phys.* **73**, 681 (2001).
- N. Dubey and M. Leclerc, *J. Polym. Sci., Part B: Polym. Phys.* **49**, 467–475 (2011).
- M. Leclerc and A. Najari, *Nat. Mater.* **10**, 409–410 (2011).
- O. Bubnova, Z. U. Khan, A. Malti, S. Braun, M. Fahlman, M. Berggren, and X. Crispin, *Nat. Mater.* **10**, 429–433 (2011).
- Y. Kim, A. Lund, H. Noh, A. I. Hofmann, M. Craighero, S. Darabi, S. Zokaie, J. I. Park, M. H. Yoon, and C. Müller, *Macromol. Mater. Eng.* **305**, 1900749 (2020).
- G.-H. Kim, L. Shao, K. Zhang, and K. P. Pipe, *Nat. Mater.* **12**, 719–723 (2013).
- A. B. Kaiser, *Rep. Prog. Phys.* **64**, 1–49 (2001).
- P. Limelette, B. Schmaltz, D. Brault, M. Gouineau, C. Autret-Lambert, S. Roger, V. Grimal, and F. Tran Van, *J. Appl. Phys.* **115**, 033712 (2014).
- D. Brault, M. Lepinoy, P. Limelette, B. Schmaltz, and F. Tran Van, *J. Appl. Phys.* **122**, 225104 (2017).
- A. M. Glauddell, J. E. Cochran, S. N. Patel, and M. L. Chabiny, *Adv. Energy Mater.* **5**, 1401072 (2015).
- V. Vijayakumar, Y. Zhong, V. Untilova, M. Bahri, L. Herrmann, L. Biniek, N. Leclerc, and M. Brinkmann, *Adv. Energy Mater.* **9**, 1900266 (2019).
- C. J. Boyle, M. Upadhyaya, P. Wang, L. A. Renna, M. Lu-Díaz, S. P. Jeong, N. Hight-Huf, L. Korugic-Karasz, M. D. Barnes, Z. Aksamija *et al.*, *Nat. Commun.* **10**, 2827 (2019).
- D. Scheunemann, V. Vijayakumar, H. Zeng, P. Durand, N. Leclerc, M. Brinkmann, and M. Kemerink, *Adv. Electron. Mater.* **6**, 2000218 (2020).
- H. Abdalla, G. Zuo, and M. Kemerink, *Phys. Rev. B* **96**, 241202(R) (2017).
- S. D. Kang and G. Snyder, *J. Nat. Mater.* **16**, 252–257 (2017).
- M. Lepinoy, P. Limelette, B. Schmaltz, and F. Tran Van, *Sci. Rep.* **10**, 8086 (2020).
- H. Wang, Y. Pei, A. D. LaLonde, and G. J. Snyder, *Material Design Considerations Based on Thermoelectric Quality Factor* (Springer, Berlin, Heidelberg, 2013), pp. 3–32.

²⁸G. Liebfried and E. Schlömann, *Nachr. Akad. Wiss. Gött., II. Math.-Phys. Kl.* **2A**, 71 (1954).

²⁹J. S. Dugdale and D. K. C. MacDonald, *Phys. Rev.* **98**, 1751 (1955).

³⁰D. P. Spitzer, *J. Phys. Chem. Solids* **31**, 19–40 (1970).

³¹N. F. Mott and E. A. Davis, *Electronic Processes in Non-Crystalline Materials*, 2nd ed. (Oxford University Press, 1979).